ORIGINAL PAPER

Upper limit analysis of stability of the water-resistant rock mass of a Karst tunnel face considering the seepage force

Wenlong Wu[1,2] · Xiliang Liu[1,2] · Jiaqi Guo[1,2,3] · Feiyue Sun[1,2] · Xin Huang[1,2,3] · Zhengguo Zhu[3]

Abstract

Based on the upper limit theorem of limit analysis and the Hoek-Brown failure criterion and considering the adverse influence of the seepage force, we established a stability analysis method of analyzing the water-resistant rock mass of a karst tunnel face, developed a critical safety thickness criterion for water inrush caused by the instability of the tunnel face, and conducted a sensitivity analysis of the main influencing parameters. We defined the safety coefficient (k) of the tunnel face's resistance to water-inrush instability during the tunnel excavation process and analyzed the dynamic evolution characteristics of the tunnel face's stability during the tunnel construction according to the safety coefficient. We used the method introduced in this paper to calculate the safe thickness of the water-resistant rock mass of the Xiema tunnel face in the first horizontal line of the Chongqing Expressway where it is adjacent to karst cavity 268. We compared these results with the calculation results of a method that did not consider the adverse influence of the karst water seepage force. The results showed that the safety thickness of the water-resistant rock mass calculated using the method proposed in this paper more accurately conformed to the actual situation of the project, which can more effectively ensure the construction safety of the tunnel segment adjacent to the anterior, concealed, high-pressure, water-rich karst cavity. The results of this study hold great significance for improving the predictability and targeted prevention of water-inrush disasters in karst tunnels.

Keywords Karst tunnel · Water-resistant rock mass of the tunnel face · Stability · Upper limit analysis · Hoek-Brown failure criterion · Seepage force

Introduction

About 15% of the Earth's topography is karst landforms (China Railway Eryuan Engineering Group CO. LTD 1984; Wang 2004), which are located in China, Russia, the USA, Germany, France, India, South Africa, the Balkan Peninsula, and other countries and regions. China has a vast territory, and karst topography is present throughout the country. Southwestern China has the largest contiguous area and the most strongly developed karst in the world (Li et al. 2017). In the areas with strong karst development, the limestone-dominated rock masses are corroded, eroded, and replenished by groundwater, and karst structures such as water-rich karst cavities and underground rivers are formed. In tunnel engineering, when the excavation is at a certain thickness in front of a high-pressure, water-rich karst cavity behind the tunnel face, if the construction is not stopped or measures such as pre-reinforcement are not taken, the combined effects of the hydraulic pressure and the excavation disturbance likely will cause the water-resistant rock mass of the tunnel face to collapse, resulting in a water-inrush disaster (Guo et al. 2017). Therefore, a sufficient safety thickness should be reserved to ensure the stability of the water-resistant rock mass of the tunnel face when constructing tunnels in high-risk, water-rich karst areas (Zhou et al. 2021).

At present, relevant experts and scholars have conducted a series of beneficial studies of the safety thickness of the water-resistant rock masses of the karst tunnel faces, and they have made positive progress. In combination with specific projects,

✉ Jiaqi Guo
  gjq519@163.com

1 School of Civil Engineering, Henan Polytechnic University, Jiaozuo 454000, Henan, China

2 Key Laboratory of Henan Province for Underground Engineering and Disaster Prevention, Jiaozuo 454000, Henan, China

3 State Key Laboratory of Mechanical Behavior and System Safety Traffic Engineering Structures, Shijiazhuang Tiedao University, Shijiazhuang 050043, Hebei, China

Gan et al. (2007) proposed a reasonable range of safety thicknesses for the rock wall of the karst tunnel face considering factors such as excavation relaxation, karst water-bearing fissure expansion, and ground stress, but the stability criterion was not given. Based on the theories of rock hydraulics and fracture mechanics, Li et al. (2010) analyzed the water rock-interaction mechanism of karst tunnels and the mechanical control of karst water on the stability of the surrounding rock, and they derived a semi-analytical solution expression for the minimum rock stratum water-resisting thickness of the tunnel face. Sun and Liu (2011) established a folding catastrophe model for the water-inrush instability of a tunnel face, and they derived an equation for the minimum safety thickness according to the catastrophe characteristics of water inrush resulting from tunnel face instability. Guo and Qiao (2012) analyzed the fracture propagation mechanism after the rock mass of the tunnel face became unstable under high-pressure karst water from the perspective of fracture mechanics, and they established an equation for the safety thickness of the rock mass of the tunnel face based on the critical hydraulic pressure. Peng and Liu (2015) used numerical simulations to analyze the mechanism of unstable water inrush in tunnels and to provide the safety thickness of water-resistant rock masses of karst tunnel faces for different hydraulic pressures and different surrounding rock grades. Based on model tests, Jiang et al. (2017) provided the minimum safety thickness for a water-resistant rock mass under different conditions and analyzed the influence of the law of ground pressure and karst hydraulic pressure on the stability of the tunnel face. To study the instability mechanism of the water-resistant rock mass of a tunnel face, Huang et al. (2019) established an attribute identification model for the safety thickness risk assessment of a water-resistant rock mass. Most of these described studies were based on the traditional elastic-plastic mechanical method, which uses the stress-strain method to describe the deformation and failure processes of a water-resistant rock mass and to establish the strength theory, but this does not conform to the actual situation of the rock mass. In fact, the failure of the water-resistant rock mass of a karst tunnel face is an instability phenomenon driven by energy, and its essence is the process of energy dissipation and release. Only by judging the stability of the water-resistant rock mass from the perspective of an energy balance can the stability of the water-resistant rock mass of the karst tunnel face be truly determined (Sun et al. 2021).

In recent years, the limit analysis method has been used widely to study the tunnel stability problem in karst areas because of its strict theoretical basis, clear calculation process, and accurate calculation results. Yang and Zhang (2016) used the upper-bound theorem in the limit analysis theory and the variational principle to study the failure mode of the water-resistant rock mass of a tunnel face with an anterior, concealed, water-rich karst cavity, and they developed a stability criterion for the water-resistant rock

mass of the tunnel face based on the minimum thickness. Yang et al. (2017a, b) adopted the limit analysis theory to study the factors influencing the stability of a water-resistant rock mass between a tunnel and a karst cave below it, and they derived the analytical solutions of the critical value and maximum value of the collapse thickness of the water-resistant rock mass. To study the instability and collapse of a water-resistant rock mass between a tunnel and a karst cave below it, Huang et al. (2017) used the limit analysis theory to derive the analytical expression for the collapsed surface and obtained the equation for the minimum safe thickness of the water-resistant rock mass. These described studies used limit analysis methods to analyze the stability of karst tunnel, water-resistant rock masses, but they did not consider the adverse influence of the karst water seepage force on the water-resistant rock mass. In the water-rich karst area, the seepage effect of groundwater will aggravate the instability and collapse of the water-resistant rock mass of the tunnel face, and many serious engineering problems are also caused by seepage. Therefore, in the construction of karst tunnel, the influence of groundwater seepage force cannot be ignored, and it is more consistent with the actual situation of the project to consider the seepage force to analyze the stability of the water-resistant rock mass of the tunnel face. On the basis of the upper-bound theorem of limit analysis and the Hoek-Brown failure criterion, in this study, we established a method of determining the stability of the water-resistant rock mass of a karst tunnel face considering the adverse influence of the seepage force, developed the critical safe thickness criterion for face instability and water inrush, and conducted a sensitivity analysis of the main parameters affecting the safety thickness of the water-resistant rock mass. To define the safety coefficient (k) of the tunnel face's resistance to water-inrush instability during the tunnel excavation process and to analyze the dynamic evolution characteristics of the tunnel face's stability during tunnel construction based on the safety coefficient, we took the Xiema tunnel of the first horizontal line of the Chongqing Expressway as an example for an engineering application to verify the rationality and practicability of the method proposed in this paper. The research results are of great significance to the early warning and prevention of water-inrush disasters in karst tunnel faces.

Basic principles

Upper limit theorem of the limit analysis considering the seepage force

The limit analysis theory includes the upper limit theorem and the lower limit theorem. Its notable characteristic is that the actual failure load can be calculated using this theory

regardless of how complex the geometric shape and loading conditions of the structure are. Therefore, this theory plays an important role in solving engineering stability problems (Yang et al. 2017a, b). The upper limit theorem and the lower limit theorem have their own scope of application. Compared with the lower limit theorem, the upper limit theorem considers the constitutive relationship of rock and soil in an ideal way, and the calculation results are more true and accurate. Therefore, the upper limit theorem is more suitable for the stability analysis of rock and soil, and its basic expression is as follows (Chen 2013): If the assumed maneuvers' allowable velocity field satisfies the displacement boundary conditions, the load determined by equating the internal energy dissipation rate to the external work rate must be greater than or equal to the actual load in the limit state. In this paper, we used the upper limit theorem to analyze the stability and critical safety thickness of the water-resistant rock mass of a tunnel face in a water-rich karst area. When considering the influence of the seepage force on the stability of the tunnel face, the seepage force is regarded as the external force acting on the rock and the soil skeleton. Therefore, the mathematical expression of the upper limit theorem is

$$\int_{\Omega} D\left(\dot{\varepsilon}_{ij}\right) d\Omega \geq \int_{S} T_i v_i dS + \int_{\Omega} F_i v_i d\Omega + \int_{\Omega} f_s v_i d\Omega, (i = 1, \cdots, n; j = 1, \cdots, n) \qquad (1)$$

where $D\left(\dot{\varepsilon}_{ij}\right)$ is the internal energy dissipation rate of the plastic strain rate vector; T_i and F_i are the area force and volume force, respectively; v_i is the velocity vector in the maneuvering velocity field; S and Ω are the surface area and volume of the research object, respectively; and f_s is the seepage force. The theorem needs to satisfy three basic assumptions: (1) the rock mass is an ideal elastic-plastic material; (2) it satisfies the small deformation critical failure criterion; and (3) it obeys the associated flow rule.

Hoek-Brown nonlinear failure criterion

Rock and soil are friction materials, which mainly exhibit shear failure. The linear Mohr-Coulomb failure criterion (M-C criterion) is usually used to characterize the shear strength of geotechnical materials in the engineering field. The actual relationship between the shear stress τ_n and the normal stress σ_n is nonlinear, however, and linear failure is only a special case. Since Hoek and Brown proposed the Hoek-Brown nonlinear failure criterion in 1980 (Hoek and Brown 1980a, b), their criterion has been widely used by scholars in the industry, and the Hoek-Brown failure criterion has been demonstrated to be an appropriate yield function for evaluating the strength and stability of rock masses in karst regions (Huang et al. 2017).

The two classical expressions of the Hoek-Brown failure criterion (H-B criterion) (Hoek and Brown 1997) are expressed (1) using the large principal stress and the small principal stress, and (2) using the normal stress and the shear stress. It is necessary to calculate the internal energy dissipation rate of the rock mass in the upper limit analysis of the stability of the water-resistant rock mass of a karst tunnel face, and the normal stress and shear stress parameters of the unit body should be considered when calculating the internal energy dissipation. Thus, it is convenient to use the second form of the Hoek-Brown failure criterion. Its mathematical expression is as follows (Lyu et al. 2020):

$$\tau_n = A\sigma_{ci}\left(\frac{\sigma_n - \sigma_{tm}}{\sigma_{ci}}\right)^B \left\{A, B \in (0,1), \sigma_{ci} \geq 0, \sigma_{tm} \geq 0\right\}, \qquad (2)$$

where τ_n and σ_n are the normal stress and shear stress, respectively, and the parameters A and B are dimensionless material constants that can be obtained through triaxial compression tests. When $B = 1$, the H-B criterion becomes the M-C linear yield criterion; σ_{ci} is the uniaxial compressive strength of the intact rock; and σ_{tm} is the tensile strength of the rock mass.

Critical safety thickness and criterion for unstable water inrush of the water-resistant rock mass of a tunnel face

In this paper, we combined the limit analysis and the variational principle (Fraldi and Guarracino 2009) to study the stability and critical safety thickness of the water-resistant rock mass of a karst tunnel face. By means of an upper-bound theorem and mathematical method, this method can be used to obtain the analytical expression for the discontinuity equation, which has the outstanding advantage of having no prior assumptions about the separation curve of the failure mode. In addition, it can be used to determine the failure range of the rock mass. The basic ideas used to calculate the critical safety thickness of the water-resistant rock mass of a tunnel face are as follows (Li and Yang 2018):

1. We used the boundary separation curve to establish the plane failure mode.
2. We calculated the internal energy dissipation power and the external force power on the velocity discontinuity surface based on the upper limit theorem and established the objective function.

3. We used the variational principle to calculate the objective function's extreme value and derive the analytical expression for the separation line equation.

4. Under the condition that the water-resistant rock mass is in a critical stable equilibrium state, we calculated its critical safe thickness.

Failure mode of water inrush due to the instability of the water-resistant rock mass of a tunnel face

To establish the stability analysis method for the water-resistant rock mass of a tunnel face and to determine the instability water-inrush criterion based on the critical safety thickness, in this paper, we established the failure mode of the water-resistant rock mass (Fig. 1) according to the model of Fraldi and Guarracino (2009).

In Fig. 1, H is the height of the excavated tunnel section; w is the separation layer thickness when the water-resistant rock mass is broken; S is the safety thickness of the water-resistant rock mass, which is an unknown quantity to be determined according to the limit analysis theory; f_s is the seepage force on the rock mass; p is the karst cavity pressure, which is equal to the hydrostatic pressure p_w; and L is the effective range of the karst cavity pressure. In addition, it is assumed that the karst cavity pressure is uniformly distributed perpendicular to the surface of the water-resistant rock mass, and the stress surface is simplified into a plane, that is, the dotted line in Fig. 1a coincides with the x-axis.

As shown in Fig. 1, the water-resistant rock mass of the tunnel face exhibits an overall squeezing failure mode at a speed v under various external forces, and the failure surface is composed of two separation curves $f(x)$ and $f(-x)$, which are symmetric about the y-axis. To simplify the calculation, we selected the water-resistant rock mass in the positive direction of the x-axis as the research object. We established a local coordinate system s–n (Fig. 1b) on the micro-unit of the separation layer with the tangent and the outer normal as the positive directions. Thus, the algebraic relationship between the angle θ and $f'(x)$ is as follows:

$$\begin{cases} \sin\theta = f'(x)\left[1 + f'(x)^2\right]^{-\frac{1}{2}} \\ \cos\theta = \left[1 + f'(x)^2\right]^{-\frac{1}{2}} \end{cases} \tag{3}$$

Calculation of the critical safe thickness of the water-resistant rock mass of a tunnel face

Objective function

To establish the objective function of the separation curve, we calculated the internal energy dissipation rate and the work power of the external force under the failure mode. In the process of calculating the internal energy dissipation, all of the internal energy dissipation of the water-resistant rock mass occurred in the separation layer with a thickness of w. We took the micro-unit near the separation line as the research object, and the deformation mode of the separation layer is shown in Fig. 1b. The micro-unit moves from the dotted line (state 1) to the solid line (state 2) with speed v, and the separation layer exhibits shear deformation along the tangential direction and tensile deformation along the normal direction. Therefore, the energy dissipation rate of the micro-unit can be expressed as follows (Yang and Zhang 2016):

$$D\left(\dot{\varepsilon}_{ij}\right) = l\left(\tau_n\dot{\gamma} + \sigma_n\dot{\varepsilon}\right) \tag{4}$$

where l is the area of the corresponding separation layer, which has a value of w; $\dot{\varepsilon}$ and $\dot{\gamma}$ are the positive and tangential strain rates, respectively. According to the definition of strain rate and the trigonometric function, the mathematical expressions for $\dot{\varepsilon}$ and $\dot{\gamma}$ are as follows (Yang et al. 2017a, b):

$$\begin{cases} \dot{\varepsilon} = \frac{v}{w}\left[1 + f'(x)^2\right]^{-\frac{1}{2}} \\ \dot{\gamma} = -\frac{v}{w}f'(x)\left[1 + f'(x)^2\right]^{-\frac{1}{2}} \end{cases} \tag{5}$$

Before determining the stress-strain rate relationship according to the orthogonal law, we had to obtain the plastic potential function of the material needs. On the basis of

Fig. 1 Failure mode of the water-resistant rock mass. (**a**) Failure mode. (**b**) Deformation mode of the separation layer
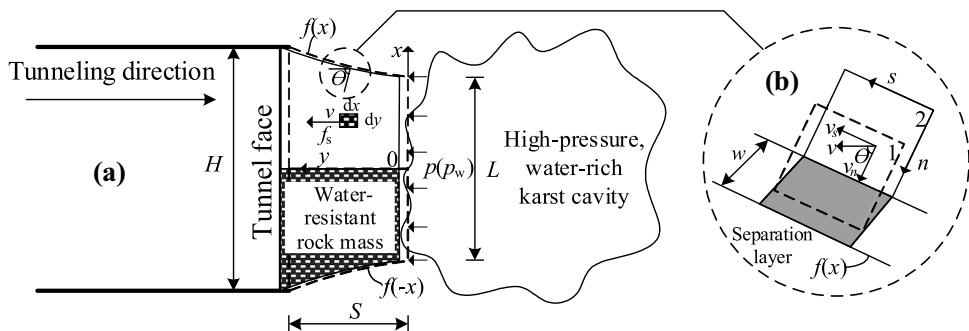
the aforementioned basic theorem, in this paper, we used the H-B failure criterion and considered the influence of the correlation flow rule. This rule not only meets the basic assumption of the limit analysis but also ensures that the yield surface coincides with the plastic potential surface. Thus, the plastic potential function $g(\sigma_n, \tau_n)$ can be expressed by the yield function $f(\sigma_n, \tau_n)$ when the material yields, and its mathematical expression is

$$g\left(\sigma_n, \tau_n\right) = f\left(\sigma_n, \tau_n\right) = \tau_n - A\sigma_{ci}\left(\frac{\sigma_n - \sigma_{tm}}{\sigma_{ci}}\right)^B \tag{6}$$

According to the orthogonal flow law, solving the derivative of the plastic potential function separately, the normal strain rate $\dot{\varepsilon}$ and $\dot{\gamma}$ the tangential strain rate $\dot{\gamma}$ can also be expressed as

$$\begin{cases} \dot{\varepsilon} = \lambda \frac{\partial g}{\partial \sigma_n} = -\lambda AB\left(\frac{\sigma_n - \sigma_{tm}}{\sigma_{ci}}\right)^{B-1} \\ \dot{\gamma} = \lambda \frac{\partial g}{\partial \tau_n} = \lambda \end{cases} \tag{7}$$

where λ is a scalar parameter. Equations (5) and (7) correspond to each other, and the expression for the normal stress σ_n can be obtained by eliminating λ and w in simultaneous Eqs. (5) and (7).

$$\sigma_n = \sigma_{ci}\left[ABf'(x)\right]^{\frac{1}{1-B}} + \sigma_{tm} \tag{8}$$

By substituting Eqs. (2), (5), and (8) into Eq. (4), the internal energy dissipation rate of the micro-unit on the separation curve $f(x)$ can be obtained, as follows:

$$D\left(\dot{\varepsilon}_{ij}\right) = l\left(\tau_n\dot{\gamma} + \sigma_n\dot{\varepsilon}\right) = v\left[1 + f'(x)^2\right]^{-\frac{1}{2}} \\ \left\{\sigma_{tm} + \sigma_{ci}\left(1 - B^{-1}\right)\left[ABf'(x)\right]^{\frac{1}{1-B}}\right\} \tag{9}$$

According to the lateral area integration formula, Eq. (9) was integrated along the total separation line, and the internal energy dissipation rate of the water-resistant rock mass was obtained:

$$\dot{W}_D = \int_\Omega D\left(\dot{\varepsilon}_{ij}\right) d\Omega = \int_{L/2}^{H/2}\left\{\sigma_{tm} + \sigma_{ci}\left(1 - B^{-1}\right)\left[ABf'(x)\right]^{\frac{1}{1-B}}\right\}v dx \tag{10}$$

Then, we calculated the work power of the external force. Under this failure mode, the external load can be divided into the karst cavity pressure, the seepage force, and the rock mass gravity. The karst cavity pressure is the surface force, and the work power can be expressed as

$$\dot{W}_{P_w} = \int_S T_i v_i dS = \frac{1}{2}pvL = \frac{1}{2}p_w vL \tag{11}$$

The gravity of the rock mass is the volume force, and it is always perpendicular to the movement direction of the rock mass. Therefore, throughout the failure process, the work done by gravity is equal to 0, that is,

$$\dot{W}_\gamma = \int_\Omega F_i v_i d\Omega = 0 \tag{12}$$

The seepage of water occurs in the pores of the water-resistant rock mass. Under the action of the water head difference, the groundwater flows through the pores of the water-resistant rock mass. Generally, the horizontal component of the tunnel face seepage force is far greater than the vertical component, so we considered only the influence of the horizontal component of the seepage force on the stability of the tunnel face (Lee and Nam 2001). The seepage force of the rock and soil mass per unit volume along the streamline direction is

$$f_s = \gamma_w i = \gamma_w \frac{\Delta h}{S} \tag{13}$$

where γ_w is the volumetric weight of the groundwater; i is the hydraulic gradient; Δh is the water head difference; and S is the seepage length, that is, the safety thickness of the water-resistant rock mass. For a rock and soil mass with volume V, the seepage force along the streamline direction is

$$F_s = \gamma_w i V = f_s V \tag{14}$$

Therefore, the power of the work done by the internal seepage force of water-resistant rock mass is

$$\dot{W}_{f_s} = \int_\Omega f_s v_i d\Omega = \int_{L/2}^{H/2}\gamma_w if(x)v dx \tag{15}$$

By substituting Eqs. (10), (11), (12), and (15) into Eq. (1), the objective function, including the separation curve $f(x)$, is obtained.

$$\xi\left[f(x), x, f'(x)\right] = \int_{L/2}^{H/2}\left\{\sigma_{tm} + \sigma_{ci}\left(1 - B^{-1}\right)\left[ABf'(x)\right]^{\frac{1}{1-B}}\right\}v dx \\ - \frac{1}{2}p_w vL - \int_{L/2}^{H/2}\gamma_w if(x)v dx \\ = \int_{L/2}^{H/2}\phi\left[f(x), x, f'(x)\right]v dx + \frac{1}{2}\sigma_{tm}v(H - L) \\ - \frac{1}{2}p_w vL \tag{16}$$

where

$$\phi\left[f(x), x, f'(x)\right] = \sigma_{ci}\left(1 - B^{-1}\right)\left[ABf'(x)\right]^{\frac{1}{1-B}} - \gamma_w if(x) \tag{17}$$

Separation curve equation

According to the basic definition of the upper limit theorem, the separation curve $f(x)$ determined by Eq. (16) is a series of upper limit solutions, which are greater than or equal to the real value. The optimal upper-bound solution can be obtained by optimizing the objective function. As evident from Eqs. (16) and (17), the extreme value of the objective function ξ is completely determined by the function φ. Therefore, solving for the extreme value of ξ also solves for the extreme value of φ. According to the variational principle, it can be transformed into a Euler equation, so that the extreme value problem can be transformed to solve the definite solution of the Euler equation under the boundary conditions. The Euler equation of φ is

$$\frac{\partial \phi}{\partial f(x)} - \frac{\mathrm{d}}{\mathrm{d}x}\left[\frac{\partial \phi}{\partial f'(x)}\right] = 0 \tag{18}$$

According to the form of Eq. (18), the function φ is simplified respectively.

$$\frac{\partial \phi}{\partial f(x)} = -\gamma_w i \tag{19}$$

$$\frac{\partial \phi}{\partial f'(x)} = -\frac{\sigma_{ci}(AB)^{\frac{1}{1-B}}}{B} f'(x)^{\frac{B}{1-B}} \tag{20}$$

$$\frac{\mathrm{d}}{\mathrm{d}x}\left[\frac{\partial \phi}{\partial f'(x)}\right] = -\frac{\sigma_{ci}(AB)^{\frac{1}{1-B}}}{1-B} f'(x)^{\frac{2B-1}{1-B}} f''(x) \tag{21}$$

Equations (19) and (21) are substituted into Eq. (18), and after sorting and simplifying, the following equation is obtained:

$$f''(x)^{\frac{2B-1}{1-B}} f''(x) = \frac{\gamma_w i(1-B)}{\sigma_{ci}(AB)^{\frac{1}{1-B}}} \tag{22}$$

By solving this second-order differential equation, the expression for the separation curve $f(x)$ can be obtained:

$$f(x) = A^{-\frac{1}{B}}\left(\frac{\gamma_w i}{\sigma_{ci}}\right)^{\frac{1-B}{B}}\left(x - \frac{C_1}{\gamma_w i}\right)^{\frac{1}{B}} + C_2 \tag{23}$$

where C_1 and C_2 are undetermined constants. According to the mechanical boundary conditions, the micro-unit located at the interface between the separation curve and the water-filled karst cavity was selected for the mechanical analysis, as shown in Fig. 2.

The mechanical equilibrium equation was established in the vertical direction. After deriving and simplifying the equation, the mathematical expression for the shear stress τ_{yx} is
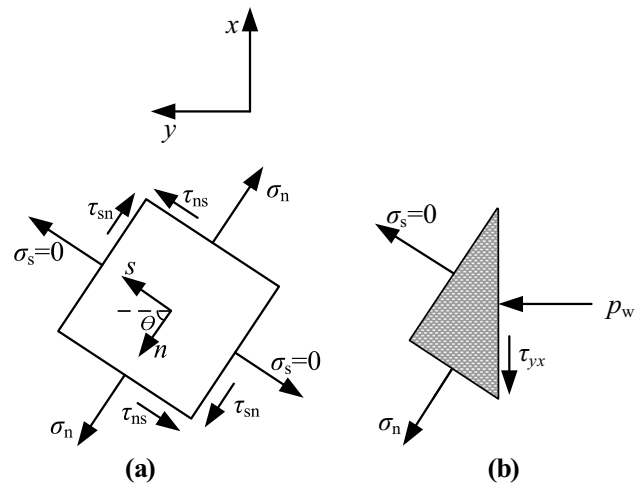
Fig. 2 Mechanical analysis of the micro-unit. **a** Located at the separation curve. **b** Located at the junction between the separation curve and the water-filled karst cavity

$$\tau_{yx} = \frac{\sigma_n \sin 2\theta}{2} - \tau_n \cos 2\theta \tag{24}$$

According to the assumption that the karst cavity pressure is uniform and is vertically distributed, there is no shear stress on the surface of the karst cavity, so τ_{yx} is 0 at $(x = L/2, y = 0)$. It can be concluded that

$$C_1 = \frac{\gamma_w i L}{2} \tag{25}$$

According to the geometric relationship of the failure modes in Fig. 1a, it is known that

$$f\left(x = \frac{L}{2}\right) = 0 \tag{26}$$

With the simultaneous Eqs. (23), (25), and (26), the value of C_2 can be obtained as 0. Therefore, the expression for $f(x)$ can be simplified to

$$f(x) = A^{-\frac{1}{B}}\left(\frac{\gamma_w i}{\sigma_{ci}}\right)^{\frac{1-B}{B}}\left(x - \frac{L}{2}\right)^{\frac{1}{B}} \tag{27}$$

Taking the separation curve as a generatrix rotating around the y-axis, the expression for the discontinuous surface formed by the failure of the water-resistant rock mass can be obtained:

$$f(x, z) = A^{-\frac{1}{B}}\left(\frac{\gamma_w i}{\sigma_{ci}}\right)^{\frac{1-B}{B}}\left(\sqrt{x^2 + z^2} - \frac{L}{2}\right)^{\frac{1}{B}} \tag{28}$$

Critical safety thickness of a water-resistant rock mass

According to the geometric relationship between the failure mode in Fig. 1a and the expression for the separation curve $f(x)$, the following equation can be obtained:

$$f\left(x = \frac{H}{2}\right) = S = A^{-\frac{1}{B}} \left(\frac{\gamma_w i}{\sigma_{ci}}\right)^{\frac{1-B}{B}} \left(\frac{H}{2} - \frac{L}{2}\right)^{\frac{1}{B}} \tag{29}$$

By substituting the hydraulic gradient $i = \Delta h / S$ and $\Delta h = p_w / \gamma_w$ into Eq. (29), the expression for the critical safety thickness of the water-resistant rock mass based on the Hoek-Brown failure criterion can simplified to

$$S_{cr} = A^{-1} \left(\frac{p_w}{\sigma_{ci}}\right)^{1-B} \left(\frac{H}{2} - \frac{L}{2}\right) \tag{30}$$

where the parameter L is an unknown number. In this case, the critical safe thickness of the water-resistant rock mass can be calculated according to the principle of virtual work in the limit analysis theory. Because the internal energy dissipation rate is equal to the power done by the external force, $\xi[f(x), x, f'(x)] = 0$ is known. Therefore,

$$\int_{L/2}^{H/2} \left\{ \sigma_{tm} + \sigma_{ci}\left(1 - B^{-1}\right)\left[ABf'(x)\right]^{\frac{1}{1-B}} \right\} v dx = \frac{1}{2} p_w v L + \int_{L/2}^{H/2} \gamma_w i f(x) v dx \tag{31}$$

and Eq. (31) simplifies to

$$(1+B)^{-1} \sigma_{ci}^{\frac{B-1}{B}} \left(\frac{p_w}{AS}\right)^{\frac{1}{B}} \left(\frac{H}{2} - \frac{L}{2}\right)^{\frac{1+B}{B}} + \frac{p_w L}{2} = \sigma_{tm}\left(\frac{H}{2} - \frac{L}{2}\right) \tag{32}$$

When the basic parameters are determined, the effective action range L of the cavity pressure can be obtained using simultaneous Eqs. (30) and (32). Thus, the critical safety thickness of the water-resistant rock mass conforming to the Hoek-Brown failure criterion can be obtained by substituting L into Eq. (30).

Criterion for water inrush due to the unstable water-resistant rock mass of a tunnel face

When a high-pressure water-rich karst cavity develops in front of a karst tunnel face and the tunnel excavation is advanced to within a certain distance from the anterior, concealed karst cavity, the excavation should be stopped immediately, and the construction plan should be changed or corresponding engineering measures should be taken to ensure the safety of the construction personnel and to prevent damage to the equipment (Xu et al. 2020; Li et al. 2021). According to the previous analysis, when the tunnel construction is stopped, the distance between

the tunnel face and the anterior, concealed karst cavity is the critical safety thickness S_{cr} of the water-resistant rock mass of the karst tunnel face. Assuming that the distance between the karst tunnel face and the anterior concealed karst cavity is S_p, the criterion for water inrush resulting from an unstable water-resistant rock mass of a karst tunnel face based on the critical safety thickness is as follows (Guo et al. 2019):

$$S_p \geq S_{cr} \tag{33}$$

Parameter sensitivity analysis

The calculation parameters have different degrees of influence on the failure range of the water-resistant rock mass, and the sensitivity analysis of the parameters holds great engineering significance to the field design and construction process (Yang and Long 2015). On the basis of the previous theoretical equation, the main parameters affecting the safety thickness of the water-resistant rock mass of a tunnel face are the compressive strength σ_{ci} and tensile strength σ_{tm} of the water-resistant rock mass, the karst water pressure p_w, the tunnel section's height H, and parameters A and B. We analyzed the influences of the changes in these parameters on the safety thickness of the water-resistant rock mass.

Compressive strength σ_{ci}

The compressive strength σ_{ci} of the water-resistant rock mass was 30–70 MPa, and the tensile strength σ_{tm} was 1/40 of the compressive strength. The karst water pressure was 1.0 MPa; the tunnel section's height was 10 m; and parameters A and B were 0.4 and 0.7, respectively. The calculation results for the safety thickness are presented in Table 1.

To more clearly determine how the safety thickness of the water-resistant rock mass changes with increasing compressive strength, we combined the typical data in Table 1 with the separation curve and the separation surface equation, and drew the failure shape and damage range of the water-resistant rock mass as two-dimensional (2D) and three-dimensional (3D) model diagrams (Fig. 3).

As shown in Table 1 and Fig. 3, when the compressive strength increased step by step from 30 to 70 MPa, the safety thickness of the water-resistant rock mass gradually decreased from 3.87 to 1.61 m, that is, the safety thickness decreased as the compressive strength of the

Table 1 Safety thickness of the water-resistant rock mass for different compressive strengths

σ_{ci} (MPa)	σ_{tm} (MPa)	p_w (MPa)	H (m)	A	B	$L/2$ (m)	S_{cr} (m)
30	0.75	1.0	10	0.4	0.7	0.70	3.87
40	1.0	1.0	10	0.4	0.7	1.46	2.93
50	1.25	1.0	10	0.4	0.7	1.99	2.33
60	1.5	1.0	10	0.4	0.7	2.38	1.92
70	1.75	1.0	10	0.4	0.7	2.69	1.61

water-resistant rock mass increased. The greater the compressive strength of the water-resistant rock mass, to a certain extent, the better the quality of the rock mass; and the higher the quality of the water-resistant rock mass, the smaller the required safety thickness of the water-resistant rock mass of the tunnel face, which was consistent with the actual situations of the engineering projects.

Tensile strength σ_{tm}

We set the compressive strength σ_{ci} of the water-resistant rock mass at 20 MPa and calculated the tensile strength σ_{tm} as 3.5/100 to 5/100 of the compressive strength. The karst water pressure was 1.0 MPa; the tunnel section's height was 10 m, and parameters A and B were 0.4 and 0.7, respectively. The calculation results for the safety thickness are presented in Table 2.

The influence of the tensile strength on the failure shape and damage range of the water-resistant rock mass is shown in Fig. 4.

As shown in Table 2 and Fig. 4, when the tensile strength of the rock mass decreased from 1.0 to 0.7 MPa, the safety thickness of the water-resistant rock mass increased from 3.61 to 4.59 m. In other words, the safety thickness increased as the tensile strength of the water-resistant rock mass decreased. Similar to the compressive strength, the smaller the tensile strength of the water-resistant rock mass, to a certain extent, the worse the quality of the rock mass; and the lower the quality of the water-resistant rock mass, the larger the required safety thickness of the water-resistant rock mass of the tunnel face, which was consistent with the actual situations of the engineering projects.

Karst water pressure p_w

In this paper, we found the karst water pressure p_w to have two effects on the water-resistant rock mass of the tunnel face: a pushing effect and a drag effect. At present, there is no unified regulation as to how the karst water
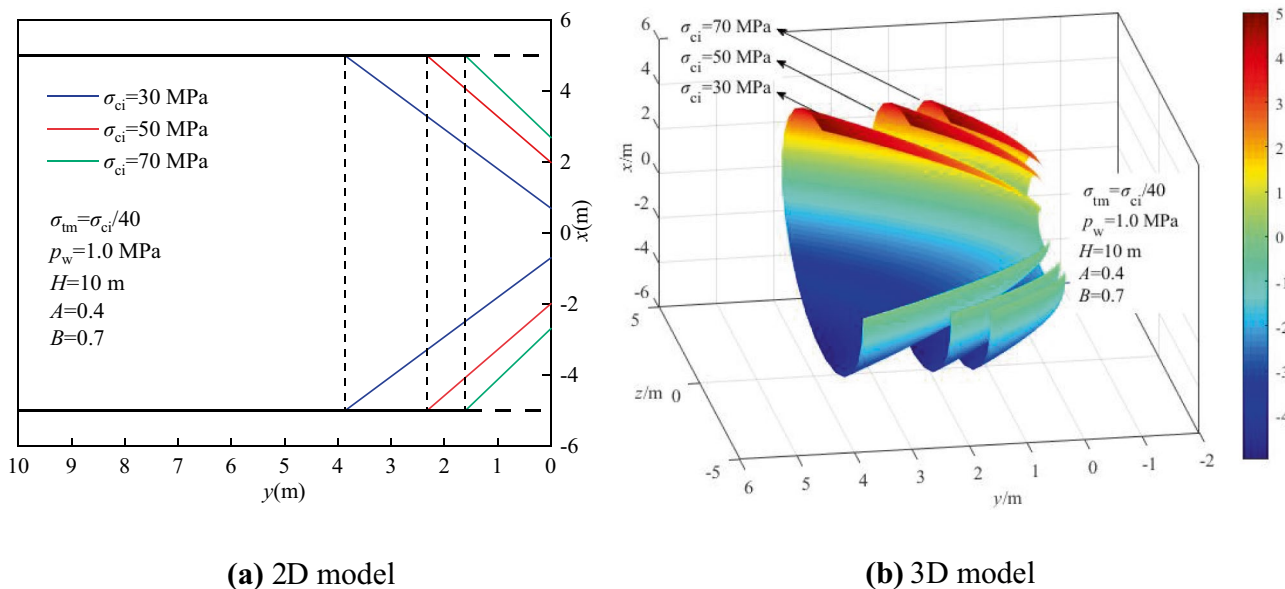
(a) 2D model

(b) 3D model

Fig. 3 Influence of the compressive strength on the failure shape and damage range of the water-resistant rock mass. **a** 2D model. **b** 3D model

Table 2 Safety thickness of the water-resistant rock mass for different tensile strengths

σ_{ci} (MPa)	σ_{tm} (MPa)	p_w (MPa)	H (m)	A	B	$L/2$ (m)	S_{cr} (m)
20	1.0	1.0	10	0.4	0.7	1.46	3.61
20	0.93	1.0	10	0.4	0.7	1.27	3.80
20	0.85	1.0	10	0.4	0.7	1.04	4.04
20	0.78	1.0	10	0.4	0.7	0.80	4.28
20	0.7	1.0	10	0.4	0.7	0.50	4.59

pressure should be classified, but scholars in the engineering industry generally agree on the following divisions (Huang 2018). Water pressures of 0.015–0.5 MPa are defined as common ordinary water pressures of a tunnel; water pressures of 0.5–1.0 MPa are common medium water pressures; water pressures of 1.05–1.5 MPa are common high-water pressures; water pressures of 1.5–5 MPa are uncommon high-water pressures; and water pressures of greater than 5 MPa are rare high-water pressures. The karst water pressure plays an important role in determining the safety thickness of the water-resistant rock mass. In this study, we calculated the karst water pressure p_w to be 1.5–3.5 MPa. The compressive strength σ_{ci} of the water-resistant rock mass was 30 MPa; the tensile strength σ_{tm} was 2.2 MPa; the tunnel section's height was 10 m; and parameters A and B were 0.5 and 0.8, respectively. The calculation results for the safety thickness are presented in Table 3.

The influence of the karst water pressure on the failure shape and damage range of the water-resistant rock mass is shown in Fig. 5.

As shown in Table 3 and Fig. 5, when the karst water pressure increased step by step from 1.5 to 3.5 MPa, the safety thickness of the water-resistant rock mass gradually increased from 2.88 to 6.06 m, that is, the safety thickness increased with increasing karst water pressure. As the karst water pressure p_w increased, the pushing and drag effects on the water-resistant rock mass increased, and thus, the degree of damage done to the water-resistant rock mass significantly increased. Therefore, the safety thickness of the water-resistant rock mass must be increased to ensure the safety of the construction site.

Tunnel excavation section height *H*

The size of the tunnel excavation section directly affected the difficulty of the construction process, and the excavation height had an important influence on the self-stability of the water-resistant rock mass of the tunnel face. In this paper, we set the height of the excavated section of the tunnel as 11–15 m for the calculations. The compressive
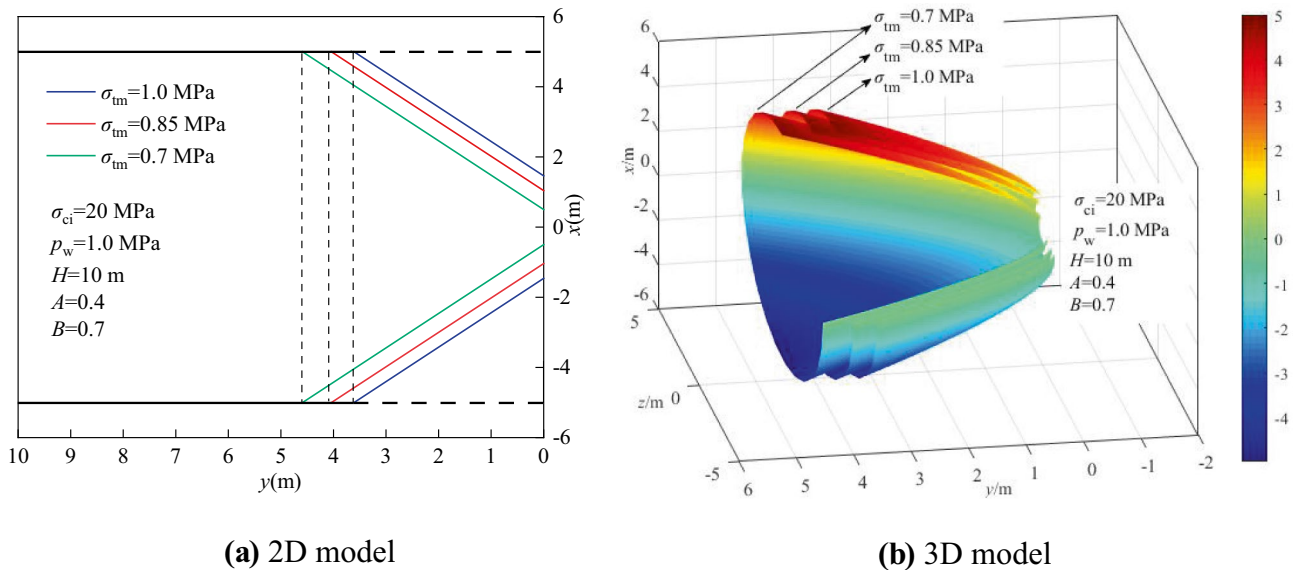
(a) 2D model

(b) 3D model

Fig. 4 Influence of the tensile strength on the failure shape and damage range of the water-resistant rock mass. **a** 2D model. **b** 3D model

Table 3 Safety thickness of the water-resistant rock mass for different karst water pressures

σ_{ci} (MPa)	σ_{tm} (MPa)	p_w (MPa)	H (m)	A	B	$L/2$ (m)	S_{cr} (m)
30	2.2	1.5	10	0.5	0.8	2.38	2.88
30	2.2	2.0	10	0.5	0.8	1.76	3.77
30	2.2	2.5	10	0.5	0.8	1.22	4.59
30	2.2	3.0	10	0.5	0.8	0.75	5.36
30	2.2	3.5	10	0.5	0.8	0.34	6.06

strength σ_{ci} of the water-resistant rock mass was 30 MPa; the tensile strength σ_{tm} was 0.75 MPa; the karst water pressure was 1.0 MPa; and parameters A and B were 0.4 and 0.7, respectively. The calculation results for the safety thickness are presented in Table 4.

The influence of the tunnel excavation section's height on the failure shape and damage range of the water-resistant rock mass is shown in Fig. 6.

As shown in Table 4 and Fig. 6, when the tunnel excavation section's height increased from 11 to 15 m, the safety thickness of the water-resistant rock mass increased from 4.26 to 5.81 m, that is, the safety thickness increased with increasing tunnel excavation height. Therefore, the larger the section height of the tunnel, the worse the self-stability of the water-resistant rock mass. In this case, a sufficient rock mass thickness should be reserved to ensure the safety of the construction process.

Parameter *A*

Parameter A is a scale parameter that controls the shear strength of the water-resistant rock mass (Yang et al. 2017a, b), and its value ranges from 0 to 1. For the calculations in this paper, we set the value of A to 0.5–0.9. The compressive strength σ_{ci} of the water-resistant rock mass was 30 MPa; the tensile strength σ_{tm} was 0.75 MPa; the karst water pressure was 1.0 MPa; the tunnel section height was 10 m; and parameter B was 0.8. The calculation results of safety thickness are shown in Table 5.

The influence of parameter A on the failure shape and damage range of the water-resistant rock mass is shown in Fig. 7.

As shown in Table 5 and Fig. 7, when the value of parameter A increased from 0.5 to 0.9, the safety thickness of the water-resistant rock mass decreased from
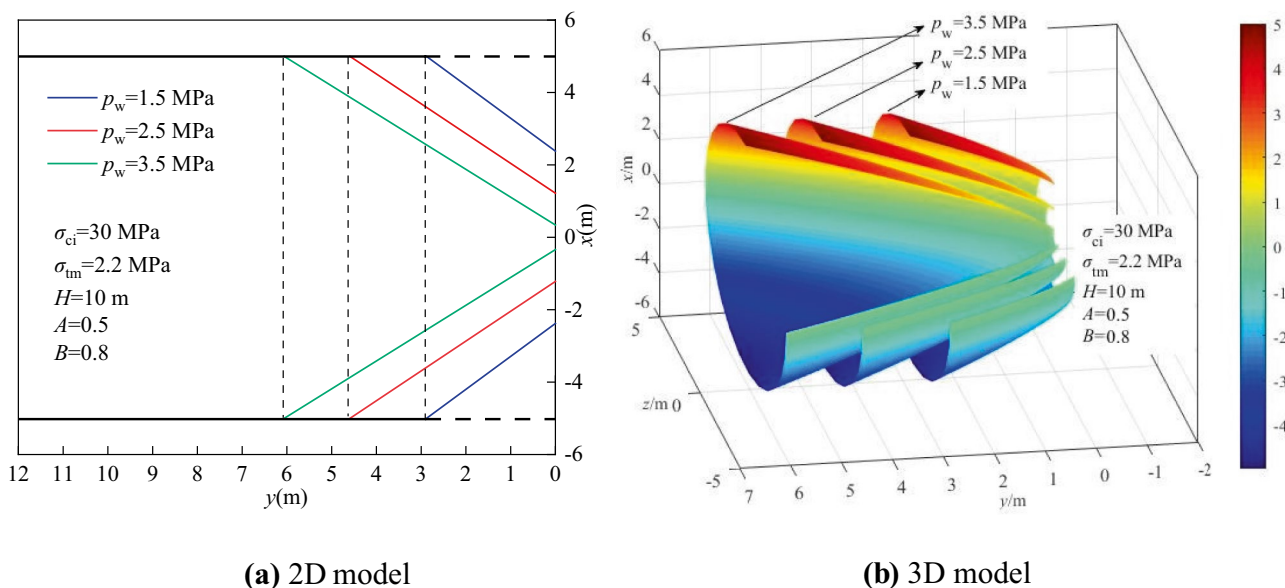
(a) 2D model

(b) 3D model

Fig. 5 Influence of the karst water pressure on the failure shape and damage range of the water-resistant rock mass. **a** 2D model. **b** 3D model

Table 4 Safety thickness of the water-resistant rock mass for different excavation section heights

σ_{ci} (MPa)	σ_{tm} (MPa)	p_w (MPa)	H (m)	A	B	$L/2$ (m)	S_{cr} (m)
30	0.75	1.0	11	0.4	0.7	0.77	4.26
30	0.75	1.0	12	0.4	0.7	0.84	4.64
30	0.75	1.0	13	0.4	0.7	0.91	5.03
30	0.75	1.0	14	0.4	0.7	0.97	5.43
30	0.75	1.0	15	0.4	0.7	1.04	5.81

4.24 to 2.36 m, that is, the safety thickness decreased as the value of parameter A increased. According to the equation for the critical safety thickness of the water-resistant rock mass of a tunnel face derived in this paper, the safety thickness was inversely proportional to parameter A. When the value of parameter A increased, the safe thickness of the water-resistant rock mass decreased accordingly.

Parameter *B*

Parameter B is the control parameter of the Mohr intensity envelope's curvature, and its value ranges from 0 to 1. The curvature radius of shear stress was smaller than the radius of the tangential Mohr circle when $B < 0.5$, so the value of parameter B should be greater than or equal to 0.5 (Yang et al. 2017a, b). For the calculations in this paper, we set the value of B to 0.5–0.9. The compressive strength σ_{ci} of the water-resistant rock mass was 30 MPa; the tensile strength σ_{tm} was 0.75 MPa; the karst water pressure was 1.0 MPa; the tunnel section's height was 10 m; and parameter A was

0.5. The calculation results for the safety thickness are presented in Table 6.

The influence of parameter B on the failure shape and damage range of the water-resistant rock mass is shown in Fig. 8.

As shown in Table 6 and Fig. 8, when parameter B increased from 0.5 to 0.9, the safety thickness of the water-resistant rock mass increased from 1.69 to 5.82 m, that is, the safety thickness increased as the value of parameter B increased. According to the equation for the critical safety thickness of the water-resistant rock mass of a tunnel face derived in this paper, the safety thickness was directly proportional to parameter B. When the value of the parameter B increased, the safe thickness of the water-resistant rock mass increased accordingly.

To sum up, the safety thickness decreased as the compressive strength, the tensile strength of the water-resistant rock mass, and parameter A increased, and it increased as the karst water pressure, the tunnel excavation height, and parameter B increased. Comparing the influence of the changes of various parameters on the safety thickness
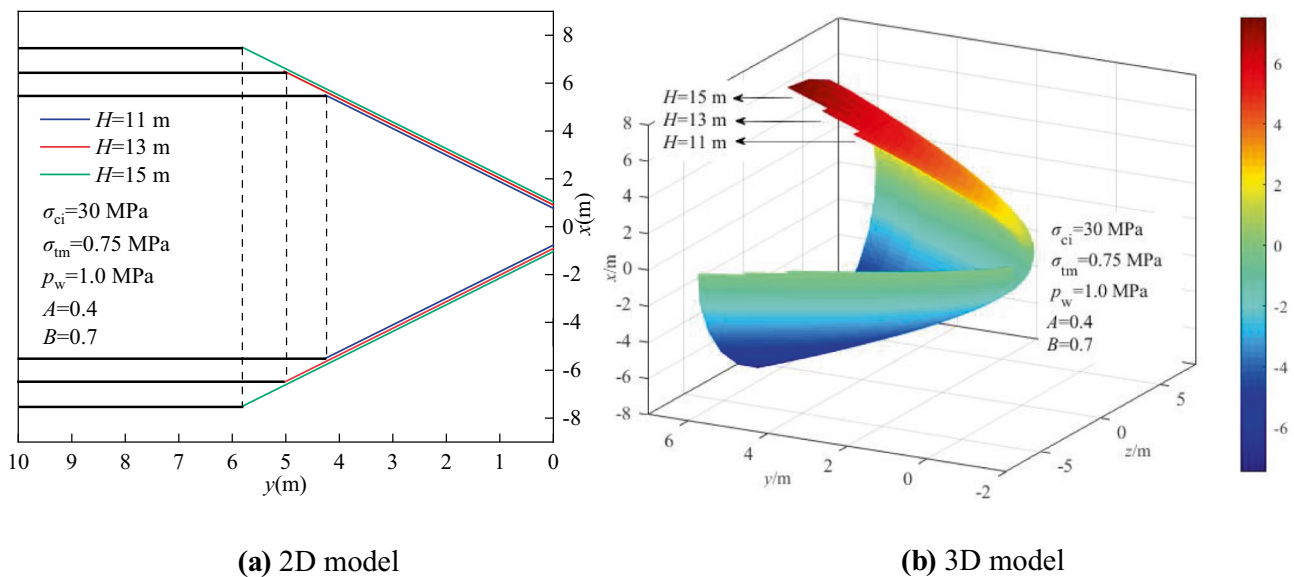
(a) 2D model   **(b)** 3D model

Fig. 6 Influence of the excavation section heights on the failure shape and damage range of the water-resistant rock mass. **a** 2D model. **b** 3D model

Table 5 Safety thickness of the water-resistant rock mass for different values of parameter A

σ_{ci} (MPa)	σ_{tm} (MPa)	p_w (MPa)	H (m)	A	B	$L/2$ (m)	S_{cr} (m)
30	0.75	1.0	10	0.5	0.8	0.81	4.24
30	0.75	1.0	10	0.6	0.8	0.81	3.54
30	0.75	1.0	10	0.7	0.8	0.81	3.03
30	0.75	1.0	10	0.8	0.8	0.81	2.65
30	0.75	1.0	10	0.9	0.8	0.81	2.36

of the water-resistant rock mass, the change of tensile strength has the weakest influence on the safety thickness, that is, the sensitivity of this parameter is poor, while the change of parameter B has the most significant influence on the safety thickness, indicating that the sensitivity of the parameter is strong.

Dynamic evolution analysis of stability of the water-resistant rock mass of a tunnel face

On the basis of the internal energy dissipation rate and the power of the work done by the external forces on the water-resistant rock mass of the tunnel face, in this paper, we defined the safety coefficient (k) of the instability of the water-resistant rock mass of the tunnel face during the tunnel excavation process. We used this coefficient to analyze the dynamic evolution process of the stability of the water-resistant rock mass of a karst tunnel face. Based on the preceding analysis, when the internal energy dissipation rate of a system was greater than or equal to the power of the work done by the external forces on the

system, the system was in a stable state. Therefore, the safety coefficient k is

$$k = \frac{\dot{W}_D}{\dot{W}_E} \geq 1 \tag{34}$$

where $\dot{W}_D$ is the internal energy dissipation rate of the rock mass reserved for the purpose of outburst prevention, and $\dot{W}_E$ is the power of the work done by the external forces on the rock mass retained for the purpose of outburst prevention. We selected corresponding parameters (i.e., $\sigma_{ci} = 100$ MPa, $\sigma_{tm} = 5$ MPa, $p_w = 1.0$ MPa, $H = 10$ m, $A = 0.2$, and $B = 0.9$) to calculate the dissipated internal energy, the work done by the external forces, and the safety factors of water-resistant rock masses of different thicknesses. The calculation results are presented in Table 7.

According to the calculation results, the dynamic evolution process of the stability of the water-resistant rock mass of the tunnel face is plotted, as shown in Fig. 9.

As shown in Table 7 and Fig. 9, as the excavation of the tunnel progressed, the distance between the tunnel face and the rock wall of the anterior concealed karst cave
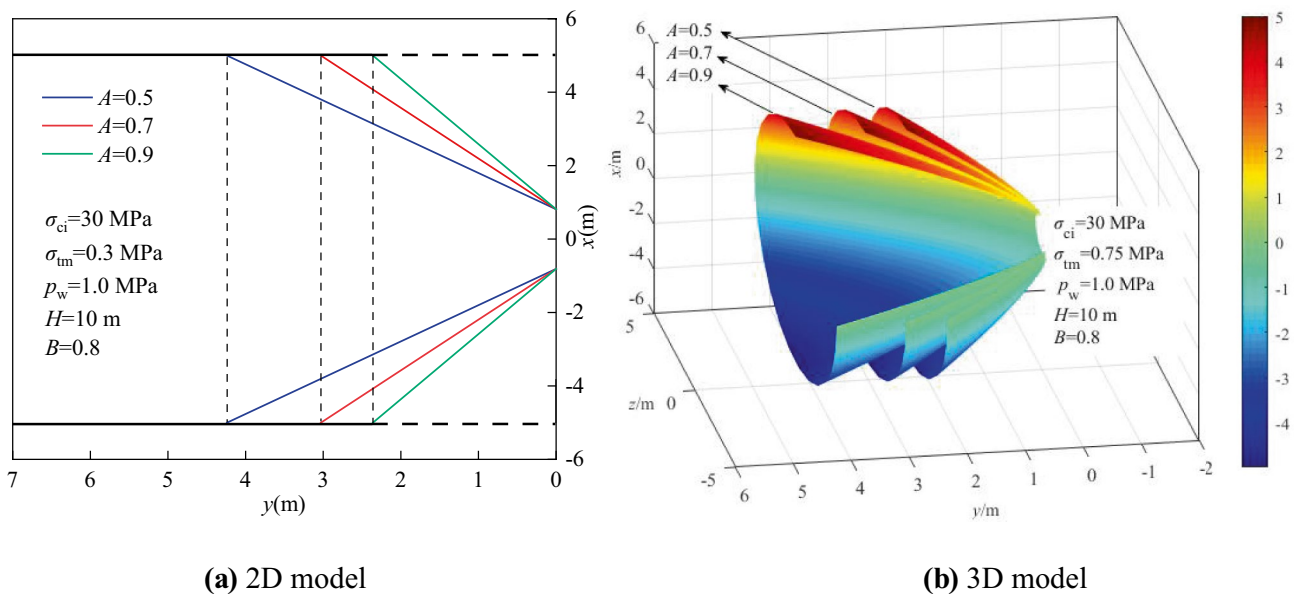
(a) 2D model

(b) 3D model

Fig. 7 Influence of the value of parameter A on the failure shape and damage range of the water-resistant rock mass. **a** 2D model. **b** 3D model

Table 6 Safety thickness of the water-resistant rock mass for different values of parameter B

σ_{ci} (MPa)	σ_{tm} (MPa)	p_w (MPa)	H (m)	A	B	$L/2$ (m)	S_{cr} (m)
30	0.75	1.0	10	0.5	0.5	0.38	1.69
30	0.75	1.0	10	0.5	0.6	0.56	2.29
30	0.75	1.0	10	0.5	0.7	0.70	3.10
30	0.75	1.0	10	0.5	0.8	0.81	4.24
30	0.75	1.0	10	0.5	0.9	0.91	5.82

decreased (i.e., the thickness of the water-resistant rock mass decreased), the energy dissipation inside the water-resistant rock mass decreased, the work done by the external forces increased, the corresponding safety coefficient k gradually decreased, and the stability of the water-resistant rock mass of the tunnel face became worse. When the tunnel excavation reached the point at which the thickness of the water-resistant rock mass was 3 m, the safety coefficient was $k = 1.04$. In this case, the water-resistant rock mass was close to the critical instability state, so the construction must continue with care. When the construction reached the point at which the thickness of the water-resistant rock mass was 2 m, the work done by the external forces on the water-resistant rock mass increased to 4666.67 J, which was greater than its dissipative internal energy (3117.04 J), and the safety coefficient was $k = 0.67$. Under these circumstances, the water-resistant rock mass of the tunnel face was destroyed, and a water-inrush disaster would occur (Fig. 9g).

When the dissipative internal energy of the water-resistant rock mass of the tunnel face was reduced to 4522.04 J, and the work done to the external forces increased to 4521.65 J, the two curves intersected. That is, the internal energy dissipation rate of the water-resistant rock mass was equal to the power of the work done by the external forces, and the safety coefficient was $k = 1$ (Fig. 9h). At this time, the water-resistant rock mass transitions from a safe stable state to a critical instability state. The water-resistant rock mass's thickness ($S = 2.87$ m) was the critical safety thickness S_{cr} of the water-resistant rock mass of the tunnel face. Therefore, during the tunnel construction process, when the water-resistant rock mass appears obvious water seepage and rock collapse phenomenon, that is, the safety coefficient is very close to 1 or equal to 1. The excavation should be stopped immediately at this time, and engineering reinforcement measures should be taken to ensure the safety of the construction site. In conclusion, the actual distance S_p between the tunnel face and
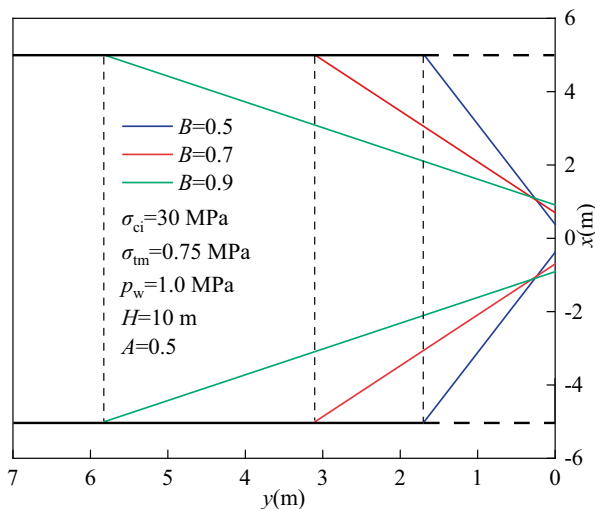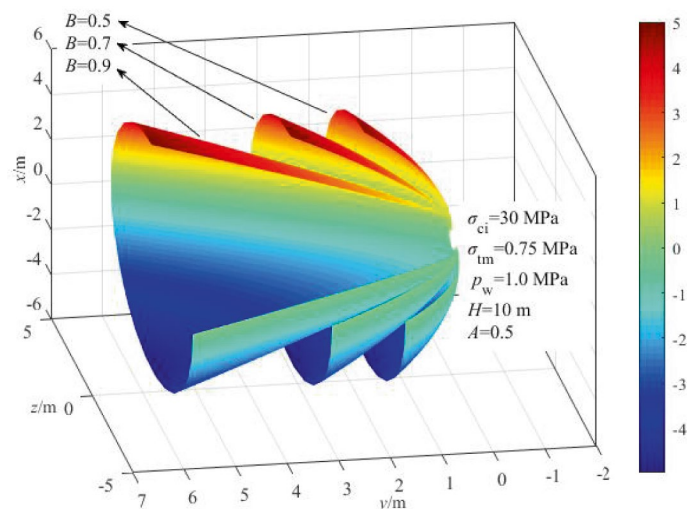
(a) 2D model **(b)** 3D model

Fig. 8 Influence of the value of parameter B on the failure shape and damage range of the water-resistant rock mass. **a** 2D model. **b** 3D model

Table 7 The dissipated internal energy, the work done by the external force and the safety coefficient for different water-resistant rock mass thicknesses

Thickness of the water-resistant rock mass (m)	10	8	6	5	4	3	2	2.87
Dissipated internal energy (J)	15,682.99	12,565.9	9400.02	7865.91	6282.97	4700	3117.04	4522.04
Work done by the external force (J)	3333.31	3666.64	3999.97	4166.66	4333.32	4499.99	4666.67	4521.65
Safety coefficient k	4.7	3.43	2.35	1.89	1.45	1.04	0.67	1

the rock wall of the anterior concealed karst cavity should be greater than or equal to the critical safety thickness S_{cr} of the water-resistant rock mass to avoid the risk of a water-inrush disaster.

Engineering application

The entrance of the Xiema tunnel of the first horizontal line of the Chongqing Expressway is located in Qiaobao, Wenfeng Village, Xiema Town, Beibei District, Chongqing, China, and the tunnel's exit is located in Nianzigang, Sanxi Village, Caijiagang Town, Beibei District. The Xiema tunnel is one of the most important municipal tunnels in Chongqing, China, and the geographic location of the tunnel is shown in Fig. 10. The total length of the Xiema tunnel is about 4200 m, and the maximum burial depth of the tunnel's roof is about 392 m, which makes it a deeply buried, extra-long tunnel. The tunnel was designed as a separate two-hole one-way three-lane tunnel with a linear tunnel body plane and a distance of 26.23–64.11 m between the two holes. The Xiema tunnel has a span of about 14.5 m and a height of about 9.6 m, and it passes through the Zhongliang Mountain area. In this area, the lithology mainly includes limestone, dolomite, argillaceous rock, and sandstone. There is abundant groundwater, well-developed karst fissures, and complex geological structures, and geological disasters such as water inrush often occur. The geological cross section of the tunnel is shown in Fig. 11 (Li et al. 2019; Yang et al. 2019). The geological exploration report shows that the right line (YK8 + 988 to YK9 + 371) of the tunnel is located in a karst development area, and there are many sinkholes and corrosion depressions on the surface. The saturated uniaxial compressive strength of the limestone is 34.36 MPa, the tensile strength is 0.888 MPa, and the integrity coefficient is 0.68. This information is relatively complete, so it is comprehensively defined as grade III surrounding rock. The groundwater activity state involves large amounts of gushing water and water jets, and the water pressure is 1.24 MPa. On August 29, 2015, a water-inrush event

occurred when the right line of the tunnel was excavated to mileage marker number YK9 + 268. The volume of the instantaneous water inflow was about 7000 m^3, and the total water output reached 4000 m^3/d after it stabilized (Wang 2018). Through advanced drilling, a water-bearing karst cave (i.e., karst cave 268) was identified behind the tunnel face. The location of this cave is shown in Fig. 11. Karst cave 268 is mainly filled with karst water. A sketch of the section of the Xiema tunnel adjacent to karst cave 268 is shown in Fig. 12. We selected the corresponding Hoek-Brown failure criterion parameters ($A = 0.3$ and $B = 0.7$) to calculate the safety thickness of the water-resistant rock mass of the tunnel face (Hoek and Brown 1997; Yang and Zhang 2016).

We substituted various parameters into Eqs. (30) and (32) and used the method introduced in this paper to calculate the safety thickness of the water-resistant rock mass of the tunnel face of the section of the Xiema tunnel adjacent to karst cavity 268. The result of the calculations was 5.24 m. Using a method that did not consider the adverse influence of the karst water seepage force, the safety thickness of the water-resistant rock mass of the tunnel face (Yang and Zhang 2016) was calculated to be 4.61 m. In the actual project, where the Xiema tunnel is adjacent to karst cavity 268, the range of the reserved safety thickness of the water-resistant rock mass of the tunnel face is 4.5–5.5 m, and the average safety thickness is 5 m. Thus, the value of the water-resistant safety thickness calculated considering the adverse influence of the karst water seepage force was closer to the actual reserved thickness of the water-resistant rock mass of the tunnel face in the project. This indicated that the safety thickness was sufficient to ensure the safety of the tunnel where it was adjacent to karst cavity 268. In summary, it was feasible to analyze the stability of the water-resistant rock mass of a tunnel face using the method introduced in this paper, and the seepage effect of the groundwater in karst areas had a significant influence on the stability of the water-resistant rock mass of a tunnel face. When tunnel construction is carried out in water-rich karst areas, the adverse influence of the karst water seepage force must be fully considered.

Fig. 9 The dynamic evolution process of stability of the water-resistant rock mass of the tunnel face: **a** $S=10$ m, **b** $S=8$ m, **c** $S=6$ m, **d** $S=5$ m, **e** $S=4$ m, **f** $S=3$ m, **g** $S=2$ m, **h** $S=2.87$ m
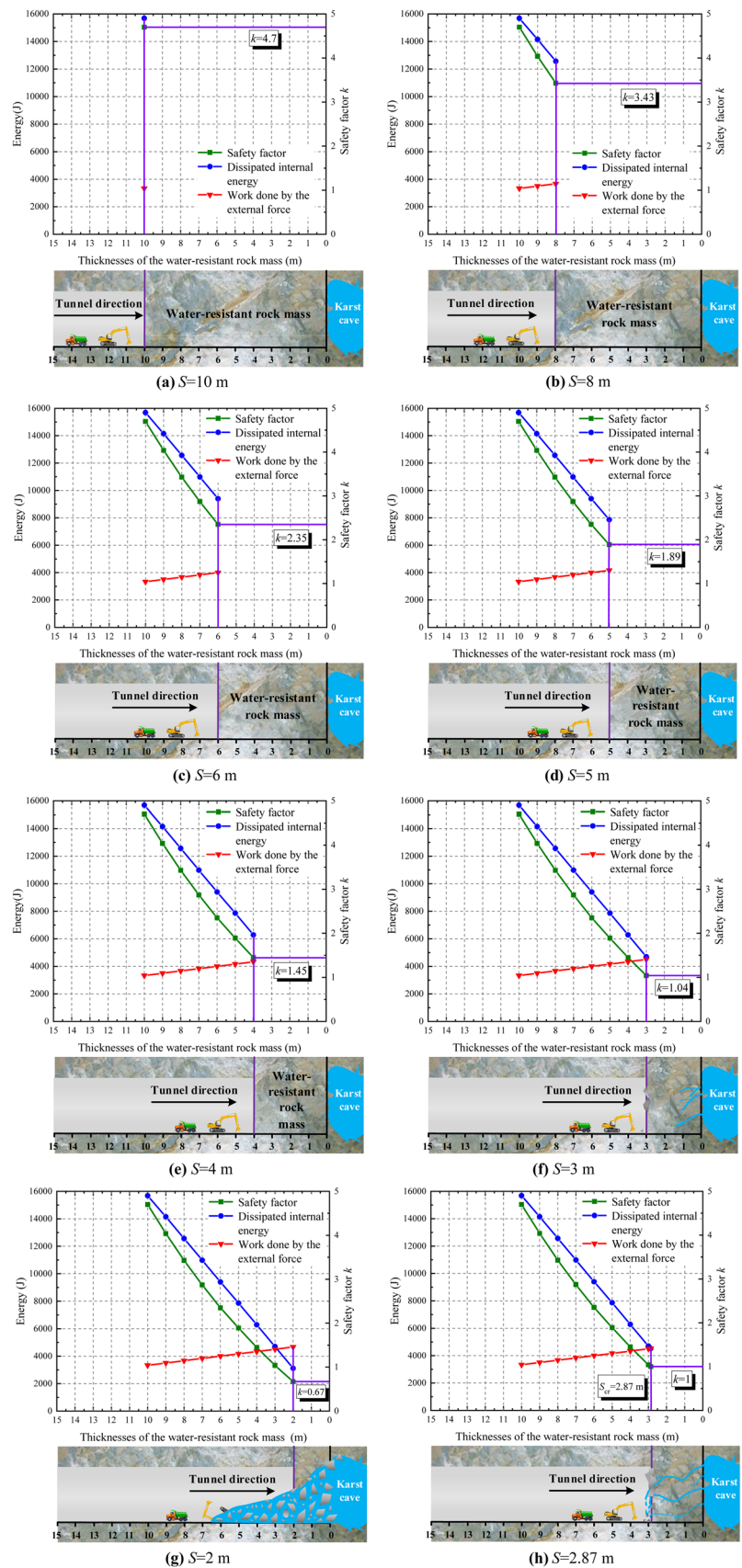
Fig. 10 Geographic location of the Xiema tunnel
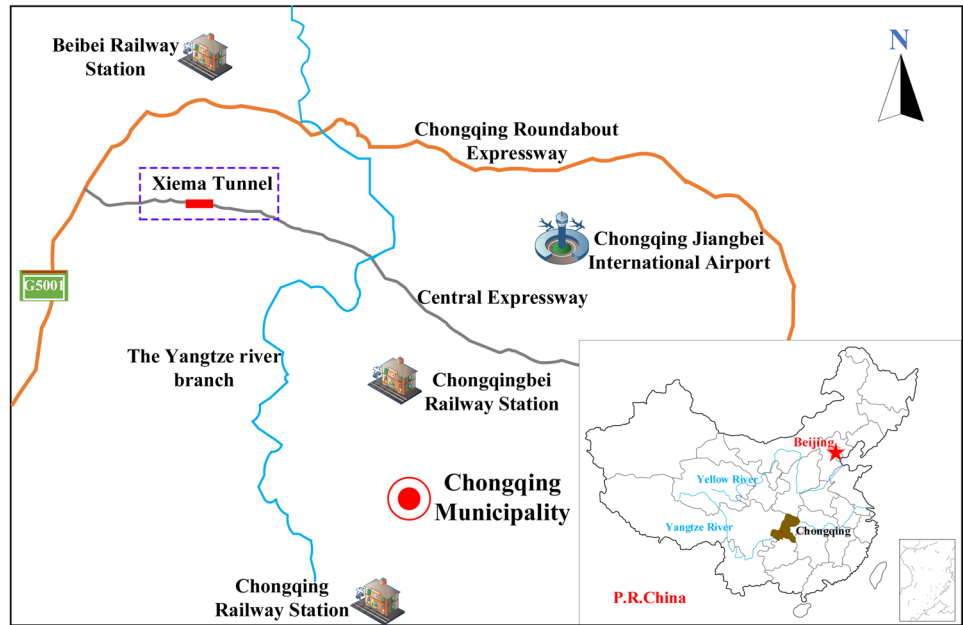
Fig. 11 Geologic cross section of the Xiema tunnel and location of karst cave 268

J$_2$x Xintiangou Formation	T$_1$J Jialingjiang Formation
J$_1$z Zhenzhuchong Formation	T$_1$f^4 Feixianguan Formation-Member 4
T$_3$xj Xujiahe Formation	T$_1$f^3 Feixianguan Formation-Member 3
T$_2$l Leikoupo Formation	T$_1$f^2 Feixianguan Formation-Member 2
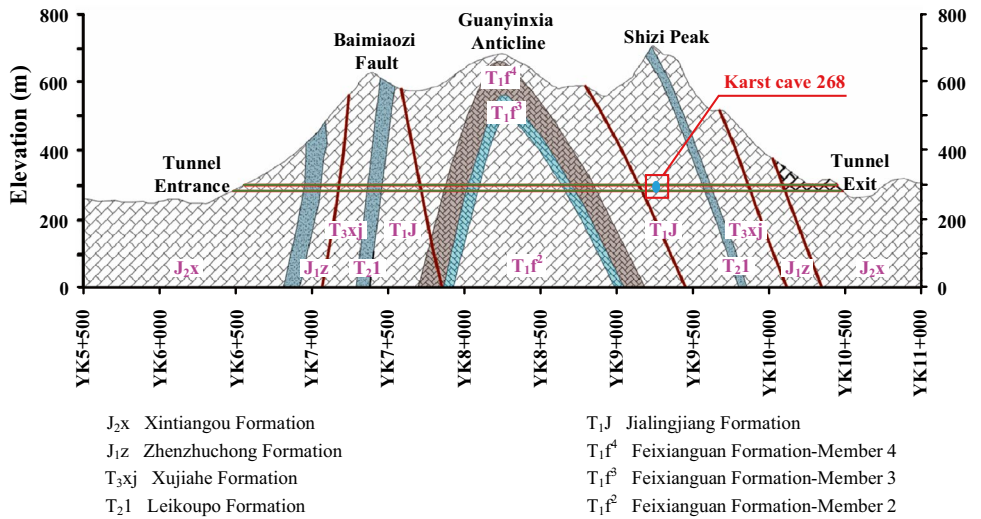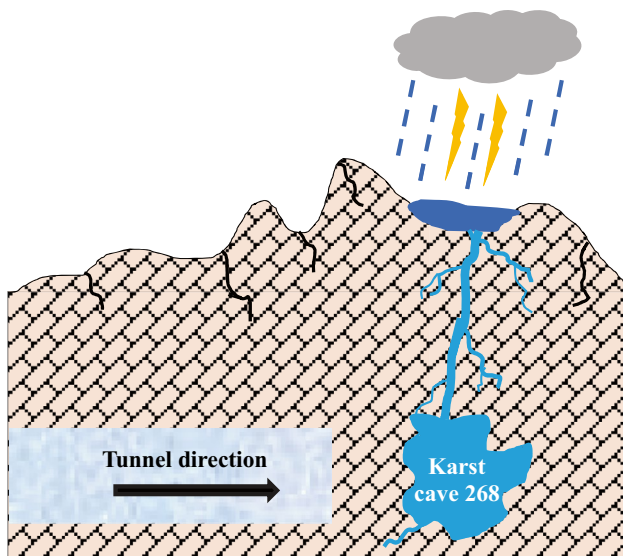
Fig. 12 Construction sketch of the section of the Xiema tunnel adjacent to karst cave 268

Conclusions

1. On the basis of the upper-bound theorem of limit analysis and the Hoek-Brown failure criterion and considering the adverse influence of the karst water seepage force, we derived an equation for the critical safety thickness of the water-resistant rock mass of a tunnel face from the perspective of energy dissipation; established a method of analyzing the stability of the water-resistant rock mass of a karst tunnel face; and developed the water-inrush instability criterion for the water-resistant rock mass of a tunnel face based on the critical safety thickness.

2. On the basis of the method to analyze the stability of the water-resistant rock mass of a karst tunnel face and considering the adverse influence of the seepage force, we conducted a sensitivity analysis of the main parameters affecting the stability of the water-resistant rock mass of the tunnel face. We determined that the safety thickness of the water-resistant rock mass of the tunnel face decreased as the compressive strength, tensile strength, and parameter A increased; and it increased as the karst water pressure, tunnel excavation height, and parameter B increased.

3. On the basis of the internal energy dissipation rate and the power of the work done by the external forces on the water-resistant rock mass of the tunnel face, we defined the safety coefficient (k) of the tunnel face's resistance to water-inrush instability during tunnel excavation. Using the safety coefficient, we analyzed the dynamic evolution characteristics of the tunnel face's stability during tunnel construction. We determined that as the tunnel excavation progressed, the energy dissipation inside the water-resistant rock mass decreased, the work done by the external forces increased,

the value of k gradually decreased, and the stability of the water-resistant rock mass became worse.

4. Taking the Xiema tunnel project of the first horizontal line of the Chongqing Expressway as an example, this paper introduced a method to calculate the safety thickness of the water-resistant rock mass of the tunnel face where the tunnel is adjacent to karst cavity 268. We compared the result with the calculation results of a method that did not consider the adverse influence of the karst water seepage force. The results revealed that the thickness of the water-resistant rock mass calculated by the method introduced in this paper was more consistent with the actual situation of the project. Thus, the proposed method better ensured the safety of tunnels constructed adjacent to anterior, concealed, high-pressure, water-rich karst cavities.

Declarations

Conflict of interest The authors declare no competing interests.

References

Chen WF (2013) Limit analysis and soil plasticity. Elsevier, Netherland

China Railway Eryuan Engineering Group CO. LTD (1984) Karst engineering geology. China Railway Press, Beijing (in Chinese)

Fraldi M, Guarracino F (2009) Limit analysis of collapse mechanisms in cavities and tunnels according to the Hoek-Brown failure criterion. Int J Rock Mech Min 46(4):665–673

Gan KR, Yang Y, Li JS (2007) Analysis on karst water inflow mechanisms and determination of thickness of safe rock walls: case study on a tunnel. Tunn Constn 27(3): 13–16, 50 (in Chinese)

Guo JQ, Li HF, Chen F, He ZY (2017) Theoretical analysis on water-resisting thickness of karst tunnel face. Chin J Underground Space Eng 13(5):1373–1380 (in Chinese)

Guo JQ, Qian Y, Chen JX, Chen F (2019) The minimum safe thickness and catastrophe process for water inrush of a karst tunnel face with multi fractures. Processes 7:686

Guo JQ, Qiao CS (2012) Study on water-inrush mechanism and safe thickness of rock wall of karst tunnel face. J China Railw Soc 34(3):106–111 (in Chinese)

Hoek E, Brown ET (1997) Practical estimates of rock mass strength. Int J Rock Mech Min 34(8):1165–1186

Hoek E, Brown ET (1980a) Underground excavations in rock. Institute of Miningand Metallurgy, London

Hoek E, Brown ET (1980b) Empirical strength criterion for rock masses. J Geotech Geoenviron 106(GT9):1013–1035

Huang F, Zhao LH, Ling TH, Yang XL (2017) Rock mass collapse mechanism of concealed karst cave beneath deep tunnel. Int J Rock Mech Min 91:133–138

Huang SW (2018) Analysis method of tunnel inrush disaster. Science Press, Beijing (in Chinese)

Huang X, Li SC, Xu ZH, Gao M, Shi XS, Gao B, Zhang B, Liu L (2019) An attribute recognition model for safe thickness assessment between concealed karst cave and tunnel. J Cent South Univ 26(4):955–969

Jiang HM, Li L, Rong XL, Wang MY, Xia YP, Zhang ZC (2017) Model test to investigate water proof-resistant slab minimum safety thickness for water inrush geohazards. Tunn Undergr Sp Tech 62:35–42

Lee IN, Nam SW (2001) The study of seepage forces acting on the tunnel lining and tunnel face in shallow tunnels. Tunn Undergr Sp Tech 16:31–40

Li LP, Li SC, Zhang QS (2010) Study of mechanism of water inrush induced by hydraulic fracturing in karst tunnels. Rock Soil Mech 31(2):523–528 (in Chinese)

Li SC, Wu J, Xu ZH, Zhou L, Zhang B (2017) A possible prediction method to determine the top concealed karst cave based on displacement monitoring during tunnel construction. B Eng Geol Environ 78:341–355

Li SC, Gao CL, Zhou ZQ, Li LP, Wang MX, Yuan YC, Wang J (2019) Analysis on the precursor information of water inrush in karst tunnels: a true triaxial model test study. Rock Mech Rock Eng 52:373–384

Li TZ, Yang XL (2018) Reliability analysis of tunnel face in broken soft rocks using improved response surface method. Int J Geomech 18(5):04018021

Li LP, Shang CS, Chu KW, Zhou ZQ, Song SG, Liu ZH, Chen YH (2021) Large-scale geo-mechanical model tests for stability assessment of super-large cross-section tunnel. Tunn Undergr Sp Tech 109:103756

Lyu C, Yu L, Wang MN, Xia PX, Sun Y (2020) Upper bound analysis of collapse failure of deep tunnel under karst cave considering seismic force. Soil Dyn Earthq Eng 132:106003

Peng J, Liu XY (2015) Water-Inrush mechanism during construction and determination of safety distance from the water source in a karst tunnel. Electron J Geotech Eng 20(8):2345–2354

Sun M, Liu WN (2011) Research on water inrush mechanism induced by karst tunnel face with high risk. Rock Soil Mech 32(4):1175–1180 (in Chinese)

Sun SQ, He P, Wang G, Li WT, Wang HB, Chen DY, Xu F (2021) Shape characterization methods of irregular cavity using Fourier analysis in tunnel. Math Comput Simulat 187:191–214

Wang H (2018) Study on the stability of surrounding rock safety thickness for the water-filling cast cave in front of the tunnel, Shandong University (in Chinese)

Wang MS (2004) Hydrologic and geological forecast of tunnel construction in the karst district. Railw Inv Survey (1): 7–9, 18 (in Chinese)

Xu ZH, Huang X, Li SC, Lin P, Shi XS, Wu J (2020) A new slice-based method for calculating the minimum safe thickness for a filled-type karst cave. B Eng Geol Environ 79:1097–1111

Yang XL, Long ZX (2015) Roof collapse of shallow tunnels with limit analysis method. J Cent South Univ 22:1926–1936

Yang ZH, Zhang JH (2016) Minimum safe thickness of rock plug in karst tunnel according to upper bound theorem. J Cent South Univ 23:2346–2353

Yang XL, Li ZW, Liu ZA, Xiao HB (2017a) Collapse analysis of tunnel floor in karst area based on Hoek-Brown rock media. J Cent South Univ 24:957–966

Yang ZH, Zhang R, Xu JS, Yang XL (2017b) Energy analysis of rock plug thickness in karst tunnels based on non-associated flow rule and nonlinear failure criterion. J Cent South Univ 24:2940–2950

Yang WM, Wang MX, Zhou ZQ, Li LP, Yuan YC, Gao CL (2019) A true triaxial geomechanical model test apparatus for studying the precursory information of water inrush from impermeable rock mass failure. Tunn Undergr Sp Tech 93:103078

Zhou ZQ, Li ZH, Gao CL, Zhang DS, Wang MX, Wei CC, Bai SS (2021) Peridynamic micro-elastoplastic constitutive model and its application in the failure analysis of rock masses. Comput Geotech 132:104037